Theory of two-dimensional spectroscopy with intense laser fields

Giovanni Bressan[1] and Jasper J. van Thor[1]*

1. Department of Life Sciences, Imperial College London, SW7 2AZ London, UK

*Corresponding author. J.vanthor@imperial.ac.uk

Abstract:

Two-dimensional vibrational and electronic spectroscopic observables of isotropically oriented molecular samples in solution are sensitive to laser fields intensities and polarisation. The third-order response function formalism predicts a signal which grows linearly with the field strength of each laser pulse, thus lacking a way of accounting for non-trivial intensity-depended effects, such as saturation and finite bleaching. An analytical expression to describe the orientational part of the molecular response, which in the weak-field limit becomes equivalent to a four point correlation function, is presented. Such expression is evaluated for Liouville space pathways accounting for diagonal and cross-peaks for all-parallel and cross-polarised pulse sequences, in both the weak- and strong-field conditions, *via* truncation of a Taylor series expansion at different orders. The results obtained in the strong-field conditions suggest how a careful analysis of two-dimensional spectroscopic experimental data should include laser pulse intensity considerations when determining molecular internal coordinates.

Introduction

Coherent multidimensional spectroscopies (CMDS), of which two-dimensional (2D) spectroscopies are a sub-class, emerged in the last two decades as increasingly important tools to study the dynamical evolution of molecular systems in the ultrafast timescale.[1–7]

Many successful examples of the application of two-dimensional spectroscopy to the study of molecular vibrations have been performed in the infrared (2DIR). 2DIR has been extensively applied to the investigation of vibrational dynamics of functional groups in proteins, in which the sensitivity of the amide I band to its environment allows the recovery of structural information.[8–11]

Two-dimensional spectroscopy in the near infrared, visible (2DES) and in the ultraviolet (2DUV) spectral regions has been extensively employed to observe and characterise the dynamics of delocalized excited electronic states (Frenkel excitons)[12] in photosynthetic pigment-protein complexes,[13–17] in model systems[18–21] and in organic and inorganic semiconducting materials.[22–25]

2DES of coupled molecular systems undergoing Foerster resonant energy transfer (FRET) also allows retrieval of structural information, since the energy transfer rate depends on both the interchromophoric distance and the relative orientation of the donor and acceptor transition dipoles.[20,26]

Furthermore, 2DES provides access to information on the Raman-active vibrational modes experiencing a distortion due to the electronic excitations (Tsuboi's rule) under examination and to how such vibrations can affect and mediate energy and charge transfer dynamics.[27–29]

Further insights on the interplay between electronic and vibrational degrees of freedom can be obtained by using so called "extreme cross-peak" techniques, such as two-dimensional electronic-vibrational (2DEV) or vibrational-electronic (2DVE) spectroscopies, in which a sequence of mixed visible and infrared laser pulses is employed to generate the molecular third-order response.[3,30,31]

Theoretical and computational advances have also been pivotal to the development of the field of multidimensional coherent spectroscopies,[2,32–36] providing a formalism to model the nonlinear response of a molecular system and simulation of 2D spectra to facilitate the assignment and interpretation of experimental data.

Since ultrafast coherent multidimensional spectroscopies rely on the generation and measurement of nonlinear optical signals, a key parameter that has to be taken into account when acquiring and analysing data is the magnitude of the electric field associated with each laser pulse illuminating the sample. Strong fields can significantly affect the energetic landscape and the dynamics of a molecular system *via* a multitude of field strength-dependent phenomena such as, two-, or multi-, photon absorption,[37] finite bleaching[38,39] and exciton-exciton annihilation processes.[40]

At the state of the art, theoretical approaches to numerically calculate femtosecond transient absorption (fsTA) signals in a non-perturbative framework have been proposed by Domcke *et al*.,[41,42]. Furthermore, Tan *et al*. presented a non-perturbative method to calculate two-dimensional spectroscopy signals to simulate the effect of phase-cycling on 2D datasets acquired in partially collinear geometry.[43] Recently, Cole *et al*. modeled the effect of finite pulses and of different detection schemes in two-dimensional spectroscopy by using a nonperturbative approach.[44] Nevertheless, a considerable amount of literature on coherent multidimensional spectroscopies relies on the perturbative framework of the third-order response functions, in which the amplitude of any measured signal scales linearly to the magnitude of the electric field of each laser pulse.[2,7] While this formalism is well suited to describe perturbations induced by weak fields, it clearly lacks a way of accounting for nontrivial intense-field induced photophysical phenomena, such as saturation or finite bleaches.

Estimating finite bleach effects in 2D spectra is of special interest when multidimensional spectroscopies are used to retrieve structural information, since neglecting their contribution can lead to wrong assignments of the internal molecular coordinates.

Gelin *et al*. shown how the perturbative approach is adequate to model multidimensional spectroscopic observables of experiments carried out at moderate electric field strengths,[42] although this contribution will be an useful reference for future coherent multidimensional spectroscopy experiments performed with high energy ultrashort pulses, such as the ones made available by OPCPA-based systems.[45]

This contribution aims to fill this gap, providing a model which reproduces literature results in the weak field limit, but also includes deviations from linearity which become more relevant when intense laser pulses are used to illuminate the sample.

Theoretical framework and calculations

In the following we want to derive rate equations for the density matrix elements involved in each response function (R_1-R_6 following notation introduced by Hamm and Zanni[7]) which contribute to the measured signal in a third order spectroscopy experiment, of which two-dimensional (2D) spectroscopy is the most general and comprehensive case. Our description involves one, or two, coupled, transition dipoles placed in the laboratory frame, interacting with a sequence of four, independently polarised, laser pulses.

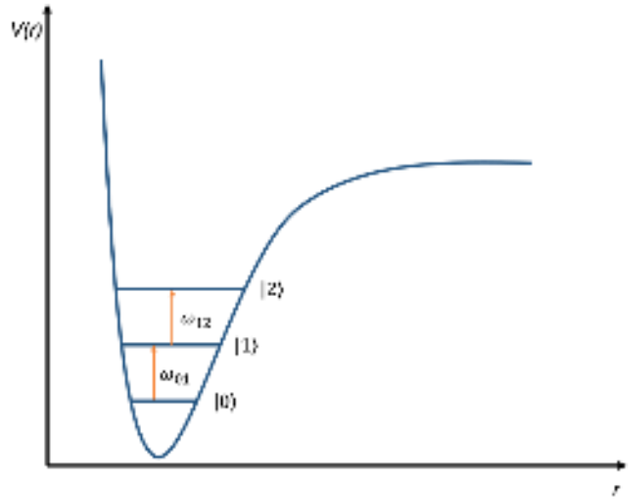

Fig. 1 Curve resulting from sectioning the anharmonic ground state potential energy surface (PES) along a given normal mode coordinate. $|0\rangle$, $|1\rangle$ *and* $|2\rangle$ *represent the ground and the first two excited vibrational levels, respectively.*

As a starting point we consider an ensemble of isotropically oriented vibrators (or oscillators) not undergoing rotational diffusion, in their ground electronic state and experiencing an anharmonic (Morse) electronic potential, as sketched in Fig. 1. The only transitions which are explicitly considered are the ones taking place between their ground and the first two vibrationally excited states, denoted as $|0\rangle$, $|1\rangle$ and $|2\rangle$, respectively (see Fig. 1). We note here that, for consistency with literature, we are modeling a 2D infrared experiment, but the same density matrix approach allows to obtain the relevant quantities for two-dimensional spectroscopy experiments in any spectral region. The 3x3 density matrix representing the isotropically oriented ensemble will look as:

$$\rho = \begin{pmatrix} \rho_{00} & \rho_{01} & \rho_{02} \\ \rho_{10} & \rho_{11} & \rho_{12} \\ \rho_{20} & \rho_{21} & \rho_{22} \end{pmatrix} \quad (1)$$

In which the diagonal terms ρ_{mm} represent populations of the *m*-th state and off-diagonal terms ρ_{mn} represent coherences between the *m*-th and *n*-th states. We can make some assumptions which will drastically reduce the number of rate equations we need to calculate, from 864 to 6.[2]
To start with, we assume that each laser pulse is weak enough to neglect two- or, in general, multi-photon absorption processes. This translates to the fact that, in a four wave-mixing experiment, it thus won't be possible to create a population in the highest-lying vibrational excited state, $\rho_{22} \equiv 0$.
Moreover, the combination of pulses giving rise to a 2D signal will have a wavevector dependance such as: $\pm k_1 \mp k_2 + k_3$, while response functions (i.e. a double-sided Feynman diagram) containing a ρ_{20} coherence will emit a double quantum (2Q) signal on a different phase-matched direction $(+k_1 + k_2 - k_3)$,[46,47] this term (and its complex conjugate) can thus be ignored. Although, the rate equation for the density matrix element of a 2Q signal can be calculated following the same approach outlined in this contribution.
Another assumption that we can make is that, at room temperature, the energy gap between the ground and first vibrationally excited states $|0\rangle$, $|1\rangle$ is considerably larger than k_BT, which is generally true for internal vibrational modes of organic molecules (as an example, the energy associated to the stretching mode of a carbonyl group is ca. $8k_BT$). This means that, prior to any field-matter interactions, we will have $\rho_{00}(-\infty) \equiv 1$. Although, calculations for pathways starting from thermally populated diagonal elements can be obtained following the procedure explained in this contribution. Finally, the off-diagonal terms above and below the diagonal are just the complex conjugate of each other, and they evolve over time with the same dynamics but with a phase-shift of π. Thus $\rho_{mn} = \rho_{nm}{}^{*}$.

The conditions stated above are used to solve the Liouville-von Neumann equation, which describes the time evolution of the system. The system Hamiltonian is $\hat{H} = \hat{H}_0 + \hat{V}(t)$, the total energy is thus given by a time independent part $\hat{H}_0$, yielding the energy of the unperturbed eigenstates, and by a time dependent part $\hat{V}(t) = -\boldsymbol{\mu_n} \cdot \boldsymbol{E_n}(t)$ which will account for the interaction energy between a transition dipole and the time-dependent electric field of the laser pulse.

We proceed by following the evolution of the density matrix elements through time for a non-rephasing stimulated emission response function, labeled as R_4 in Hamm and Zanni notation.[7] This pathway is taken as an example, but the same approach allows to calculate the time-evolution of the relevant density matrix elements for any double-sided Feynman diagram.
After the first interaction, happening at t_1, we will have an-off diagonal element whose time evolution will be:

$$\frac{\rho_{10}(t_1,\Omega)}{dt_1} = \left(-i\omega_{01} - \frac{1}{T_2}\right)\rho_{10}(t_1,\Omega) - \frac{\boldsymbol{\mu_1}}{\hbar}\boldsymbol{E_1}(t_1)\rho_{00}(-\infty,\Omega) \quad (2)$$

In which ω_{01} is a frequency proportional to the energy gap between the eigenenergies of the two diagonal elements, obtained as solution of the time independent Schroedinger equation, Ω is the solid angle element and a dephasing happening with a lifetime T_2 is phenomenologically added to describe decoherence of the off-diagonal element. The second term on the right hand side of (2) accounts for the removal of population from the ground state density matrix element, and it is explicitly written as a dot product between the molecular transition dipole and the laser pulse electric field, denoted as $\boldsymbol{\mu_1}$ and $\boldsymbol{E_1}(t_1)$, respectively. We make the implicit assumption that the frequency of the oscillating electric field is resonant with the transition we are exciting, and we recall here that the electric field can be written as $\boldsymbol{E_1}(t_1) = \boldsymbol{E'}_1(t_1) + \boldsymbol{E'^*_1}(t_1)$, with the first term oscillating at a negative frequency (so it will excite kets and de-excite bras) and the second term oscillating at a positive frequency (so it will excite bras and de-excite kets). From now on, we will keep writing the electric fields as $\boldsymbol{E_n}(t_n)$, but we will only account for their positive or negative frequency components, according to the Feynman diagram we are looking at. Equation (2) will have to be solved with the boundary condition: $\rho_{10}(t_1 = 0, \Omega) = 0$.
The first term of differential equation (2) at $t_1 = 0$ will be null, so the solution of (2) will have a form:[48]

$$\rho_{10}(t_1 = 0, \Omega) = 1 - \rho_{00}(-\infty, \Omega)e^{-\frac{1}{\hbar}\int_{-\infty}^{t_1}\boldsymbol{\mu_{10}}\boldsymbol{E_1}(t_1)dt_1} \quad (3)$$

Equation (3) can be solved for a laser pulse of arbitrary envelope (delta, gaussian, sech^2). In the simplest case of a delta-function pulse, and recalling that $\rho_{00}(-\infty) \equiv 1$ and that the dot product between two vectors can be written as the product of their modules times the cosine of their internal angle, defined as $\theta_{\mu_{10}E_1}$, we obtain:

$$\rho_{10}(t_1 = 0, \Omega) = 1 - e^{-\frac{\mu_1}{\hbar}E_1{}^0\cos\theta_{\mu_{10}E_1}} \quad (4)$$

Equation (4) shows how the magnitude of the coherent superposition created by the laser pulse perturbation, i.e. of the off-diagonal element ρ_{10} depends on the magnitude of the transition dipole (which is not an experimentally controllable parameter), on the magnitude of the electric field of the laser pulse integrated over its time duration, and on the angle between the field polarization and transition dipole vectors. In (4), $E_1{}^0$ represents the integral of the modulus of $\boldsymbol{E_n(t)}$ over the time duration of the laser pulse.
Although, (4) represents the state of the system immediately after the pulse is "turned off". In order to represent the full time evolution of ρ_{10} during the time interval between the first and the second laser pulses, we need to solve (2) after the pulse is turned off, so that Equation (2) will reduce to:

$$\frac{\rho_{10}(t_1,\Omega)}{dt_1} = \left(-i\omega_{10} - \frac{1}{T_2}\right)\rho_{10}(t_1 = 0,\Omega) \tag{5}$$

The solution of Equation (5) will yield a term oscillating at a frequency proportional to the energy splitting between $|0\rangle$, $|1\rangle$ according to the solution of the time independent part of the system Hamiltonian, and to an exponentially decaying term, representing dephasing, happening with a lifetime T_2:

$$\rho_{10}(t_1,\Omega) = (1 - e^{-\frac{\mu_1}{\hbar}{E_1}^0 \cos\theta_{\mu_{10}E_1}}) \cdot e^{-i\omega_{10}t_1}e^{-t_1/T_2} \tag{6}$$

The first term on the right-hand side of Equation (6) is equivalent to a one-point correlation function which represents the interaction of an arbitrarily oriented oscillator with an arbitrarily polarised laser pulse. The same approach can be iterated two more times to obtain an expression which accounts for the magnitude and the dynamics of the off-diagonal matrix element $\rho_{10}(t_1,t_2,t_3)$ after three laser pulse-matter interactions taking place at increasing times, as shown in (7).

$$\rho_{10}(t_1,t_2,t_3,\Omega) = (1 - e^{-\frac{\mu_1}{\hbar}{E_1}^0 \cos\theta_{\mu_{10}E_1}})(1 - e^{-\frac{\mu_2}{\hbar}{E_2}^0 \cos\theta_{\mu_{10}E_2}})(1 - e^{-\frac{\mu_3}{\hbar}{E_3}^0 \cos\theta_{\mu_{10}E_3}}) \cdot e^{-i\omega_{01}(t_1+t_3)}e^{-(t_1+t_3)/T_2} \cdot e^{-t_2/T_1} \tag{7}$$

The first three terms in Equation (7) account for the dependence of ρ_{10} on the electric field and transition dipole moment vector orientation, for a given a Liouville space pathway, while the second part of the right hand side of equation (7) contains the oscillatory and decaying (due to dephasing T_2 and population relaxation T_1) dynamics of the density matrix element.

By looking at the time dependence of (7) we can confirm that this expression, derived for R_4, describes, in fact, a non-rephasing pathway, in which the signal oscillates and decays as a function of $(t_1 + t_3)$. It can be shown that the expression for $\rho_{10}(t_1,t_2,t_3)$ obtained for the stimulated emission rephasing pathway R_2, is identical to (7), but the oscillating and dephasing terms will have a functional dependence on $(t_1 - t_3)$, which generates a "photon echo" when $(t_1 = t_3)$ and thus removes the broadening due to dephasing.[7]

It can be shown that an equation analogous to (7) for the R_6 response function, i.e. for a Liouville space pathway producing a non-rephasing excited state absorption (ESA) signal, can be obtained following the same approach. Such result is shown in Equation 7b:

$$\rho_{21}(t_1,t_2,t_3,\Omega) = (1 - e^{-\frac{\mu_1}{\hbar}{E_1}^0 \cos\theta_{\mu_{10}E_1}})(1 - e^{-\frac{\mu_2}{\hbar}{E_2}^0 \cos\theta_{\mu_{10}E_2}})(1 - e^{-\frac{\mu_3}{\hbar}{E_3}^0 \cos\theta_{\mu_{21}E_3}}) \cdot e^{-i\omega_{10}t_1}e^{-t_1/T_2} \cdot e^{-t_2/T_1} \cdot e^{-i(\omega_{10}-\Delta)t_3}e^{-t_3/T_2} \tag{7b}$$

In Equation (7b) $\Delta = (\omega_{10} - \omega_{21})$ is a positive frequency term accounting for the redshift of the oscillation frequency during the signal time due to the anharmonicity of the ground state potential energy surface (see Fig 1).

Equation (7) and (7b) can be factorised in an angular, time independent, part (its first three terms on the right hand side), whose dynamics are given by the fourth to sixth term of its right hand side. From now on we will focus on the time-independent part of Equation 7.

The emitted signal S will scale to the third order polarisation, which is proportional to: $P^{(3)} \propto \frac{\mu_4(t_4)}{\hbar}\rho_{10}(t_1,t_2,t_3,\Omega)$.[7] The third order signal in 2D experiments is either self-heterodyned[3] (in pump-probe 2D spectroscopy setups) or heterodyned by a local oscillator[49] (LO, in fully non-collinear BOXCARS-like setups). In either cases, this involves taking a projection of the third order polarisation along the heterodyning field, with electric field $E_4(t)$, or to consider the interference term arising by the transmission of the third order signal through a polariser. Treating the fourth interaction in the

same way of the first three, and including just the angular part of the fourth interaction, we obtain the following expression:

$$S(\Omega) \propto (1 - e^{-\frac{\mu_1}{\hbar}E_1{}^0 \cos\theta_{\mu_1 E_1}}) \cdot (1 - e^{-\frac{\mu_2}{\hbar}E_2{}^0 \cos\theta_{\mu_2 E_2}}) \cdot (1 - e^{-\frac{\mu_3}{\hbar}E_3{}^0 \cos\theta_{\mu_3 E_3}}) \cdot (1 - e^{-\frac{\mu_4}{\hbar}E_4{}^0 \cos\theta_{\mu_4 E_4}}) \quad (8)$$

The lowest order term of the Taylor series expansion of (8), for small values of the integrated electric field $E_n{}^0$ becomes:

$$S(\Omega) = (\cos\theta_{\mu_1 E_1}) \cdot (\cos\theta_{\mu_2 E_2}) \cdot (\cos\theta_{\mu_3 E_3}) \cdot (\cos\theta_{\mu_4 E_4}) \frac{\mu_1}{\hbar}\frac{\mu_2}{\hbar}\frac{\mu_3}{\hbar}\frac{\mu_4}{\hbar} E_1{}^0 E_2{}^0 E_3{}^0 E_4{}^0 \quad (9)$$

Which is analogous to the familiar equation for a polarization-resolved 2D response, constituted of a four-point correlation function multiplied by the magnitudes of transition dipole moments and electric fields involved in a given Liouville-space pathway, summarized a number of years ago by Hamm and Zanni.[7] Gelin *et al.* have shown how the perturbative result, analogous to Equation (9), is adequate to model ultrafast spectroscopy experiments with moderate laser pulse energies.[42]
The ensemble-averaged value of Equation 8 can then be obtained by integration over the solid angle Ω.
In this model, dynamical processes such as spectral diffusion on energy transfer are ignored. Although, since the model here presented allows to evaluate the magnitude (and the orientational distribution) of a density matrix element immediately after each field-matter interaction, dynamical processes taking place between two consecutive pulses can be introduced in a phenomenological way.

<u>One oscillator, diagonal peak, <*ZZZZ*> polarisation, no rotational diffusion:</u>

To obtain the ensemble averaged response, in the simplest case of a single oscillator, sketched in Fig. 2, interacting with an "all-parallel" pulse sequence <*ZZZZ*>, in which all pulses are vertically polarized, parallel to the Z-axis of the laboratory frame. We proceed by substituting the relevant quantities in equation (8) and then by calculating the ensemble averaged value.

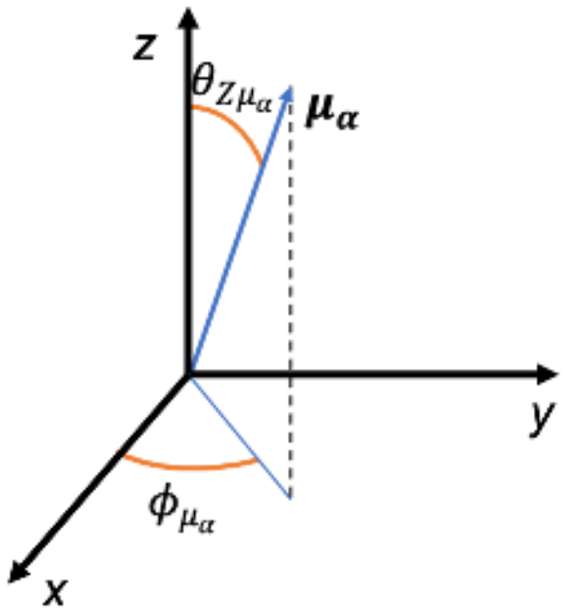

Fig. 2 The transition dipole μ_α sitting in the laboratory frame, angles $\theta_{Z\mu_\alpha}$ and ϕ_{μ_α} are indicated.

Making the assumption that the magnitude of the integrated electric field of each pulse is identical, we can write ${E_1}^0 = {E_2}^0 = {E_3}^0 = {E_4}^0 = E^0$. Furthermore, as all the transitions are involving the same transition dipole moment, we will also have $\mu_1 = \mu_2 = \mu_3 = \mu_4 = \mu^\alpha$. Equation (8) will thus become:

$$S_{ZZZZ}^{\alpha\alpha\alpha\alpha}(\Omega) = \left(1 - e^{-\frac{\mu_\alpha}{\hbar}E^0 \cos\theta_{Z\mu_\alpha}}\right)\left(1 - e^{-\frac{\mu_\alpha}{\hbar}E^0 \cos\theta_{Z\mu_\alpha}}\right)$$
$$\left(1 - e^{-\frac{\mu_\alpha}{\hbar}E^0 \cos\theta_{Z\mu_\alpha}}\right)\left(1 - e^{-\frac{\mu_\alpha}{\hbar}E^0 \cos\theta_{Z\mu_\alpha}}\right) \quad (10)$$

The ensemble averaged value of $S_{ZZZZ}^{\alpha\alpha\alpha\alpha}(\Omega)$ can be obtained by integration of (10) over the solid angle:

$$\langle S_{ZZZZ}^{\alpha\alpha\alpha\alpha}\rangle = \int S_{ZZZZ}^{\alpha\alpha\alpha\alpha}(\Omega)d\Omega = p_o \int_0^{2\pi}\int_0^{\pi}\left(1 - e^{-\frac{\mu_\alpha}{\hbar}E^0 \cos\theta_{Z\mu_\alpha}}\right)^4 sin\theta d\theta\, d\phi \quad (11)$$

In which $p_o = 1/4\pi$ is a normalisation factor for the integration in spherical coordinates. (11) can be solved analytically yielding:

$$\langle S_{ZZZZ}^{\alpha\alpha\alpha\alpha}\rangle = \frac{12\frac{\mu_\alpha}{\hbar}E^0 + 36\sinh(2\frac{\mu_\alpha}{\hbar}E^0) - 16\sinh(3\frac{\mu_\alpha}{\hbar}E^0) + 3\sinh(4\frac{\mu_\alpha}{\hbar}E^0) - 48\sinh(\frac{\mu_\alpha}{\hbar}E^0)}{12\frac{\mu_\alpha}{\hbar}E^0} \quad (12)$$

Equation (11) contains a algebraic sum of hyperbolic sine functions and thus displays saturation behaviour for strong field strength, with a threshold value of 1, which corresponds to the initial population in the ground state before any field-matter interaction. An alternative approach to solve (11) involves term by term integration over the solid angle of its Taylor series expansion, for small values of E^0. The Taylor expansion can be truncated to any arbitrary odd order. Truncation at the 5th order yields:

$$\langle S_{ZZZZ}^{\alpha\alpha\alpha\alpha Tay(5)}\rangle = \frac{\left(\frac{\mu_\alpha}{\hbar}E^0\right)^4}{5} \quad (13)$$

Which matches with the results derived by Hochstrasser[50] using a tensor approach, and then summarized by Hamm and Zanni.[7] In the weak-field approximation the molecular response is linear with respect to the electric field of each laser pulse. Although, if higher orders are included in the Taylor series expansion of (10), it is possible to account for non-trivial effects caused by the electric field strength, as shown for integration of the 7th order expansion of (10) in equation (14):

$$\langle S_{ZZZZ}^{\alpha\alpha\alpha\alpha Tay(7)}\rangle = \frac{\left(\frac{\mu_\alpha}{\hbar}E^0\right)^4\left(42 + 65\left(\frac{\mu_\alpha}{\hbar}E^0\right)^2\right)}{210} \quad (14)$$

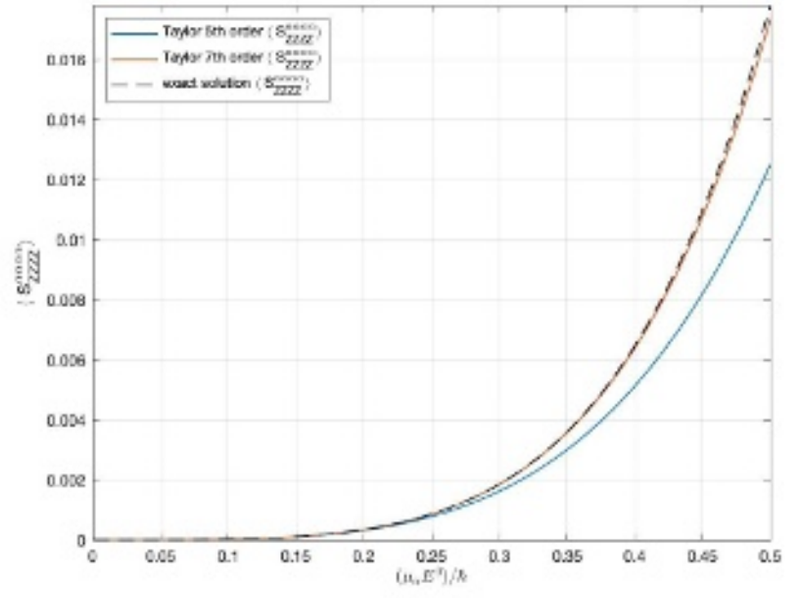

Fig. 3 Electric field-dependent signal strength for a diagonal peak due to a transition dipole interacting with an all-parallel <ZZZZ> pulse sequence. Ensemble average of the exact solution (Equation 9) is plotted as a black dashed line, and ensemble averages of the Taylor series expansion at the 5th and 7th orders, (Equations 13 and 14), are plotted as orange and blue solid lines, respectively.

The same approach is used to obtain the ensemble averaged response for the other pulse polarization combinations in the following section.

One oscillator, diagonal peak, <*ZZXX*>, <*ZXZX*>, <*ZXXZ*> polarization, no rotational diffusion:

Another pulse polarisation scheme which is commonly encountered in two-dimensional spectroscopy experiments is to have the pulses coming in pairs of mutually parallel (and thus perpendicular) polarisation. When looking at third order responses in solution, we have to recall that we are operating in a system belonging to a spherical symmetry group, thus the pulses will necessarily have to come in pairs, otherwise an odd number of cosine functions will cause the ensemble averaged integral to be equal to zero. Nevertheless, it has been shown that such condition is relaxed when operating on single crystals, in which pulse sequences as <*ZZZX*> can yield non-zero responses in low-symmetry crystal structures.[36]
However, restricting ourselves to the case of an isotropically oriented ensemble of molecules in solution, the aforementioned symmetry constraint implies that a nonzero signal amplitude will only be generated by pulse sequences such as <*ZZXX*>, <*ZXZX*> or <*ZXXZ*>. Standard manipulation of spherical coordinates allows us to write the Z and X components of μ^α as trigonometric functions of the angles $\theta_{Z\mu^\alpha}$ and ϕ_{μ^α}, thus Equation (10) becomes:

$$S^{\alpha\alpha\alpha\alpha}_{ZZXX,ZXZX,ZXXZ}(\Omega) = \left(1 - e^{-\frac{\mu_\alpha}{\hbar}E^0 \cos\theta_{Z\mu_\alpha}}\right)\left(1 - e^{-\frac{\mu_\alpha}{\hbar}E^0 \cos\theta_{Z\mu_\alpha}}\right)$$
$$\left(1 - e^{-\frac{\mu_\alpha}{\hbar}E^0 \sin\theta_{Z\mu_\alpha}\cos\phi_{\mu_\alpha}}\right)\left(1 - e^{-\frac{\mu_\alpha}{\hbar}E^0 \sin\theta_{Z\mu_\alpha}\cos\phi_{\mu_\alpha}}\right) \quad (15)$$

Taylor series expansion of (15) up to the 5th order followed by term by term integration over the solid angle, as in Equation (11), yields:

$$\langle S^{\alpha\alpha\alpha\alpha}_{ZZXX,ZXZX,ZXXZ}{}^{Tay(5)} \rangle = \frac{\left(\frac{\mu_\alpha}{\hbar}E^0\right)^4}{15} \quad (16)$$

Which, again, is in agreement with the literature results and linear with respect to the electric field strength of each laser pulse. A non-trivial dependence of the molecular response on the electric field strength of the laser pulses can be derived by truncating the Taylor series expansion of (15) at its 7th order:

$$\langle S_{ZZXX,ZXZX,ZXXZ}^{\alpha\alpha\alpha\alpha}{}^{Tay(7)} \rangle = \frac{\left(\frac{\mu_\alpha}{\hbar}E^0\right)^4 \left(2+\left(\frac{\mu_\alpha}{\hbar}E^0\right)^2\right)}{30} \tag{17}$$

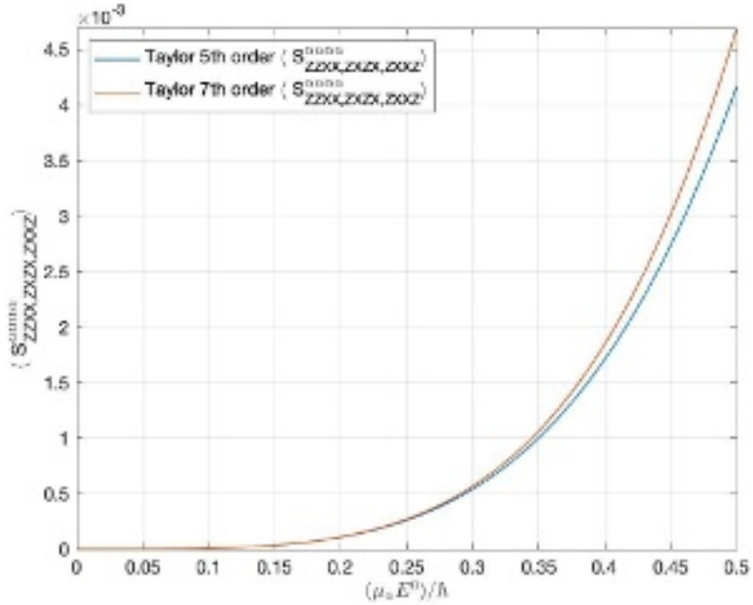

Fig. 4 Electric field-dependent signal strength for a diagonal peak due to a transition dipole interacting with a <ZZXX> ,<ZXZX> or <ZXXZ> pulse sequence. Ensemble average of the Taylor series expansion at the 5th and 7th orders (Equations 16 and 17), are plotted as blue and orange solid lines, respectively.

Two coupled oscillators, off-diagonal peak, <ZZZZ> polarisation, no rotational diffusion:

One of the distinctive features of two- and, generally speaking, multi-dimensional spectra is the presence of off-diagonal (cross) peaks which stem from the coupling between two transition dipoles. The relative amplitude of such cross peak can yield structural information, such as the relative angle between the transition dipole moments.

We will now focus on the amplitude of the cross-peaks arising from the coupling of two transition dipoles $\boldsymbol{\mu_\alpha}$ and $\boldsymbol{\mu_\beta}$ within a rigid molecule, as shown in Figure 5.

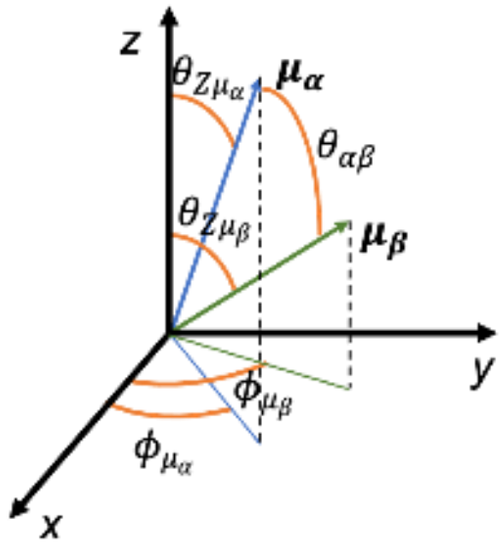

Fig. 5 Scheme of two coupled transition dipoles $\boldsymbol{\mu_\alpha}$ and $\boldsymbol{\mu_\beta}$,sketched in blue and green, respectively, belonging to the same molecular structure, sitting in the laboratory frame. Angles $\theta_{Z\mu_\alpha}$, $\theta_{Z\mu_\beta}$, ϕ_{μ_α}, $\phi_{\mu_\beta}$and $\theta_{\alpha\beta}$ are indicated.

As above, the calculation of the projections of the dipoles onto the laser pulse polarization vectors is required to model the orientational response of the system. For a <ZZZZ> sequence of all-parallel pulses, and double-sided Feynman diagrams of the type $\alpha\beta\alpha\beta$, $\alpha\alpha\beta\beta$ and $\alpha\beta\beta\alpha$, equation (10) becomes:

$$S_{ZZZZ}^{\alpha\alpha\beta\beta,\alpha\beta\alpha\beta,\alpha\beta\beta\alpha}(\Omega) = \left(1 - e^{-\frac{\mu_\alpha}{\hbar}E^0\cos\theta_{Z\mu_\alpha}}\right)\left(1 - e^{-\frac{\mu_\alpha}{\hbar}E^0\cos\theta_{Z\mu_\alpha}}\right)\left(1 - e^{-\frac{\mu_\beta}{\hbar}E^0\cos\theta_{Z\mu_\beta}}\right)\left(1 - e^{-\frac{\mu_\beta}{\hbar}E^0\cos\theta_{Z\mu_\beta}}\right) \quad (18)$$

The main constraint here is that, since the two transition dipole moments are rigidly connected $\theta_{\alpha\beta}$ is a constant. Thus, the ensemble average, which corresponds to the integral of the molecular response over all possible molecular orientations, cannot be calculated by integrating separately over the coordinates of the two coupled transition dipole moments.
To get around this, we can express $\cos\theta_{Z\mu_\beta}$ as a function of $\theta_{Z\mu_\alpha}, \phi_{Z\mu_\alpha}$ and of $\theta_{\alpha\beta}, \phi_{\alpha\beta}$, using spherical harmonics:[7]

$$\cos\theta_{Z\mu_\beta} = \frac{4\pi}{3}\left[-Y_{-1,1}(\theta_{Z\mu_\alpha}, \phi_{Z\mu_\alpha})Y_{1,1}(\theta_{\alpha\beta}, \phi_{\alpha\beta}) + Y_{1,0}(\theta_{Z\mu_\alpha}, \phi_{Z\mu_\alpha})Y_{1,0}(\theta_{\alpha\beta}, \phi_{\alpha\beta}) - Y_{1,1}(\theta_{Z\mu_\alpha}, \phi_{Z\mu_\alpha})Y_{1,-1}(\theta_{\alpha\beta}, \phi_{\alpha\beta})\right] \quad (19)$$

Equation (19) is substituted in (18) and then its Taylor series expansion, truncated at its 5th term, is integrated over the coordinates of $\boldsymbol{\mu_\alpha}$, as in Equation (11). This calculation yields:

$$\langle S_{ZZZZ}^{\alpha\alpha\beta\beta,\alpha\beta\alpha\beta,\alpha\beta\beta\alpha Tay(5)}\rangle = \frac{{\mu_\alpha}^2{\mu_\beta}^2\left(\frac{E^0}{\hbar}\right)^4}{15}\left(2\cos{\theta_{\alpha\beta}}^2 + 1\right) \quad (20)$$

Which, once again, matches literature results.[50] If the nearest nonzero higher order term is taken into account, it is possible to model non-trivial dependence of the measured response on the electric field strength of the pulses, as shown by (21). This effect can be seen as an electric field magnitude-dependent angular broadening of the bleached population (Fig.6, right panel) i.e. a finite

bleach of the isotropically oriented distribution of molecules in solution, prior to any field-matter interaction.[38,48,51]

$$\langle S_{ZZZZ}^{\alpha\alpha\beta\beta,\alpha\beta\alpha\beta,\alpha\beta\beta\alpha\,Tay(7)}\rangle = \frac{{\mu_\alpha}^2{\mu_\beta}^2\left(\frac{E^0}{\hbar}\right)^4}{15}\left(\frac{1}{8}\cos\theta_{\alpha\beta}{}^2 + \mu_\alpha\mu_\beta\left(\frac{E^0}{\hbar}\right)^2\left(\frac{1}{18}\cos\theta_{\alpha\beta}{}^3 + \frac{1}{8}\cos\theta_{\alpha\beta}{}^2 + \frac{1}{12}\cos\theta_{\alpha\beta} + \frac{1}{30}\right) + \frac{1}{15}\right) \quad (21)$$

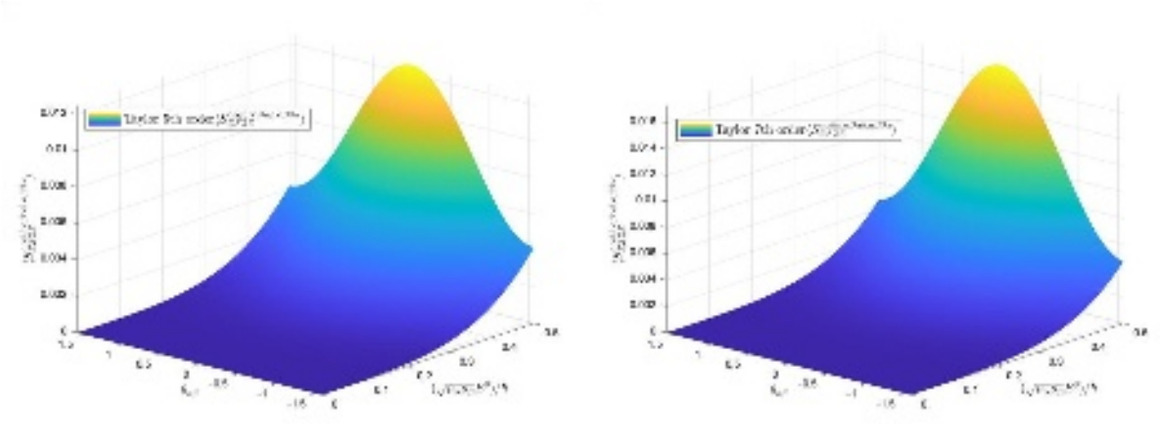

Fig. 6 Electric field-dependent signal strength for a cross-peak ($\alpha\alpha\beta\beta, \alpha\beta\alpha\beta$ or $\alpha\beta\beta\alpha$) due to two coupled transition dipoles interacting with an all-parallel <ZZZZ> pulse sequence. Ensemble averages of the Taylor series expansion at the 5th and 7th orders (Equations 20 and 21), are plotted as 3D surfaces as a function of the internal angle $\theta_{\alpha\beta}$, in the left and right panels, respectively.

Two coupled oscillators, ZZXX, ZXZX, ZXXZ polarisation, no rotational diffusion:

To retrieve structural information about the molecular system under examination, the response calculated in the previous section is not sufficient. In addition to the all-parallel pulse sequence one needs to measure a cross peak with at least one pulse sequence with orthogonally polarised pulses, such as <ZZXX>, <ZXZX> or <ZXXZ>.
Applying such polarisation schemes and the relevant double-sided Feynman diagrams to Equation (8) we obtain two more equations which need to be computed:

$$S_{X-peak\,1}^{X-pol}(\Omega) = \left(1 - e^{-\frac{\mu_\alpha}{\hbar}E^0\cos\theta_{Z\mu_\alpha}}\right)\left(1 - e^{-\frac{\mu_\alpha}{\hbar}E^0\sin\theta_{Z\mu_\alpha}\cos\phi_{\mu_\alpha}}\right)\left(1 - e^{-\frac{\mu_\beta}{\hbar}E^0\cos\theta_{Z\mu_\beta}}\right)\left(1 - e^{-\frac{\mu_\beta}{\hbar}E^0\sin\theta_{Z\mu_\beta}\cos\phi_{\mu_\beta}}\right) \quad (22)$$

$$S_{X-peak\,2}^{X-pol}(\Omega) = \left(1 - e^{-\frac{\mu_\alpha}{\hbar}E^0\cos\theta_{Z\mu_\alpha}}\right)\left(1 - e^{-\frac{\mu_\alpha}{\hbar}E^0\cos\theta_{Z\mu_\alpha}}\right)\left(1 - e^{-\frac{\mu_\beta}{\hbar}E^0\sin\theta_{Z\mu_\beta}\cos\phi_{\mu_\beta}}\right)\left(1 - e^{-\frac{\mu_\beta}{\hbar}E^0\sin\theta_{Z\mu_\beta}\cos\phi_{\mu_\beta}}\right) \quad (23)$$

It has to be noted here that the quantities $S_{X-peak\,1}^{X-pol}(\Omega)$ and $S_{X-peak\,2}^{X-pol}(\Omega)$ indicate cross-peaks due to different four-point correlation functions, rather than to distinct photophysical phenomena such as ground-state bleach (GSB), stimulated emission (SE) or excited state absorption (ESA). Namely, $S_{X-peak\,1}^{X-pol}(\Omega)$ reflects the contribution of a $(Z\cdot\alpha)(Z\cdot\beta)(X\cdot\alpha)(X\cdot\beta)$ four-point

correlation function to the total signal, while $S^{X-pol}_{X-peak\ 2}(\Omega)$ accounts for contributions arising from a $(Z\cdot\alpha)(Z\cdot\alpha)(X\cdot\beta)\ (X\cdot\beta)$ four-point correlation function.
Equations (22) and (23) will have to be integrated in order to produce an ensemble-averaged value for the third-order molecular response, but again the integration has to be performed over the coordinates of $\boldsymbol{\mu_\alpha}$, thus the need to write the product $\sin\theta_{Z\mu_\beta}\cos\phi_{\mu_\beta}$ as a function of $\theta_{Z\mu_\alpha}, \phi_{Z\mu_\alpha}$ and $\theta_{\alpha\beta}, \phi_{\alpha\beta}$. To do so, the projection over the *xy* plane of μ_β is calculated as follows:

$$\phi_{\mu_\beta} = \phi_{\mu_\alpha} - \phi_{\alpha\beta} \tag{24}$$

and then Equation (19) is plugged into the spherical law of cosines and solved for $\sin\theta_{Z\mu_\beta}$, yielding:

$$\sin\theta_{Z\mu_\beta} = \frac{\cos(\theta_{\alpha\beta})-\cos(\theta_{Z\mu_\alpha})\left(\cos(\theta_{Z\mu_\alpha})\cos(\theta_{\alpha\beta})+\frac{e^{-\phi_{\mu_\alpha}i}e^{\phi_{\alpha\beta}i}\sin(\theta_{Z\mu_\alpha})\sin(\theta_{\alpha\beta})}{2}+\frac{e^{\phi_{\mu_\alpha}i}e^{-\phi_{\alpha\beta}i}\sin(\theta_{Z\mu_\alpha})\sin(\theta_{\alpha\beta})}{2}\right)}{\cos(\phi_{\alpha\beta})\sin(\theta_{Z\mu_\alpha})} \tag{25}$$

Substitution of (24) and (25) in Equations (22) and (23), followed by their Taylor series expansion up to the 5th order, and integration over the coordinates of μ_α yield:

$$\langle S^{X-pol\ \ Tay(5)}_{X-peak\ 1}\rangle = {\mu_\alpha}^2{\mu_\beta}^2\left(\frac{E^0}{\hbar}\right)^4\left(\frac{\cos(\theta_{\alpha\beta})^2}{10}-\frac{1}{30}\right) \tag{26}$$

$$\langle S^{X-pol\ \ Tay(5)}_{X-peak\ 2}\rangle = -{\mu_\alpha}^2{\mu_\beta}^2\left(\frac{E^0}{\hbar}\right)^4\left(\frac{\cos(\theta_{\alpha\beta})^2}{15}-\frac{2}{15}\right) \tag{27}$$

Both Equations (26) and (27) are in agreement with Hochstrasser results[50] and account for the weak-field limit orientational response of two coupled dipoles interacting with a sequence of four cross-polarised pulses. Once more, ensemble average integration of the Taylor series expansions up to the 7th term of Equations (22) and (23) allows to model for a finite bleaching and saturation. The ensemble averaged value of the 7th order expansion of Equation (22) is shown in Equation (28) and plotted in the right panel of Fig. 7.

$$\begin{aligned}\langle S^{X-pol\ \ Tay(7)}_{X-peak\ 1}\rangle = {} & \frac{7{\mu_\alpha}^3{\mu_\beta}^3\left(\frac{E^0}{\hbar}\right)^6\cos(4\theta_{\alpha\beta})}{2}+168{\mu_\alpha}^2{\mu_\beta}^2\left(\frac{E^0}{\hbar}\right)^4-\frac{349{\mu_\alpha}^3{\mu_\beta}^3\left(\frac{E^0}{\hbar}\right)^6}{8}- \\ & 588{\mu_\alpha}^2{\mu_\beta}^2\left(\frac{E^0}{\hbar}\right)^4\cos(2\theta_{\alpha\beta})-132{\mu_\alpha}^3{\mu_\beta}^3\left(\frac{E^0}{\hbar}\right)^6\cos(2\theta_{\alpha\beta})-54{\mu_\alpha}^3{\mu_\beta}^3\left(\frac{E^0}{\hbar}\right)^6\cos(3\theta_{\alpha\beta})- \\ & 18{\mu_\alpha}^3{\mu_\beta}^3\left(\frac{E^0}{\hbar}\right)^6\sin(2\theta_{\alpha\beta})+21{\mu_\alpha}^3{\mu_\beta}^3\left(\frac{E^0}{\hbar}\right)^6\sin(3\theta_{\alpha\beta})+\frac{33{\mu_\alpha}^3{\mu_\beta}^3\left(\frac{E^0}{\hbar}\right)^6\sin(4\theta_{\alpha\beta})}{2}+ \\ & 84{\mu_\alpha}^2{\mu_\beta}^2\left(\frac{E^0}{\hbar}\right)^4-\frac{31{\mu_\alpha}^3{\mu_\beta}^3\left(\frac{E^0}{\hbar}\right)^6}{2}-66{\mu_\alpha}^3{\mu_\beta}^3\left(\frac{E^0}{\hbar}\right)^6\cos(\theta_{\alpha\beta})\end{aligned} \tag{28}$$

Even if the ensemble average integral of the Taylor expansion at the 7th order of Equation (23) does not have a closed form solution, that it is not needed to obtain structural information on the relative orientation of the two coupled transition dipoles when looking at cross peaks arising from rephasing Liouville-space pathways, as shown in the following section of this contribution.

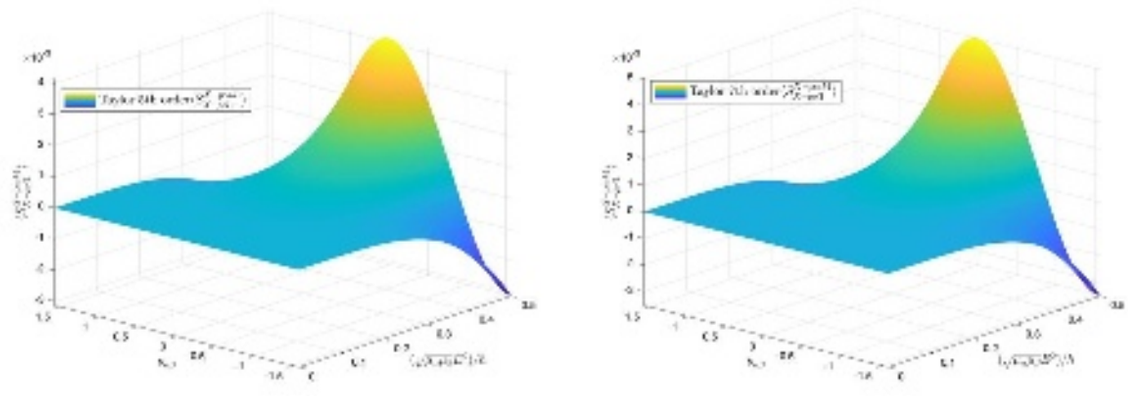

Fig. 7 Electric field-dependent signal strength for $S_{X-peak\ 1}^{X-pol}$. Ensemble averages of the Taylor series expansion at the 5th and 7th orders (Equations 26 and 28), are plotted as 3D surfaces as a function of the internal angle $\theta_{\alpha\beta}$, in the left and right panels, respectively.

Discussion

In the previous section we have shown how the model presented in this contribution allows to calculate all the equations that relate the signal strength of a diagonal and a cross peak for two coupled oscillators measured with pulse sequences with different polarization conditions. This model reproduces literature results when the ensemble average is calculated on the lowest term of the Taylor series expansion for a weak electric field, but also allows to model deviations from literature results when higher order of the expansion are integrated over the solid angle (or when the integration is).

Now such results can be used to determine the internal angle between the two coupled dipoles $\theta_{\alpha\beta}$ based on the relative strength of cross-peak signals measured with different pulse polarisation conditions.

To do so, we rescale the cross-polarised, cross-peak signal by a factor of three, to match the diagonal peaks measured with a <ZZZZ> and <ZXXZ> pulse sequence (see Equations 13 and 16) and then compute the ratio:

$$S_{ratio} = \frac{\langle S_{ZZZZ}^{\alpha\alpha\alpha\alpha,\alpha\alpha\beta\beta,\alpha\beta\beta\alpha}\rangle}{3\langle S_{X-peak\ 1}^{X-pol}\rangle} \tag{29}$$

using the ensemble averages obtained by the Taylor expansions up to the 5th (Equations (20) and (26)), and 7th orders (Equations (21) and (28)), respectively. The difference in results is evident, the ratio between 5th order expansions can be written as:

$$S_{ratio}{}^{5th\ order} = \frac{4\cos(\theta_{\alpha\beta})^2+2}{9\cos(\theta_{\alpha\beta})^2-3} \tag{30}$$

Equation (30) does not contain any electric field magnitude dependence on the signal.

To evaluate Equation (29) for the 7th order expansions of Equations (18) and (22) a rescaling factor different from 3 has to be used. Such factor can be obtained as the ratio between the signals, calculated as integration of the 7th order expansions, of a diagonal peak in all-parallel (Equation 14) and cross-polarised (Equation 17) conditions. The resulting Equation is then:

$$S_{ratio}{}^{7th\ order} = \frac{\langle S_{ZZZZ}^{\alpha\alpha\beta\beta,\alpha\beta\alpha\beta,\alpha\beta\beta\alpha\ Tay(7)}\rangle}{n_{resc}\langle S_{X-peak\ 1}^{X-pol\quad Tay(7)}\rangle} \tag{31}$$

With the normalization factor n_{resc}defined as:

$$n_{resc} = \frac{\langle S_{ZZZZ}^{\alpha\alpha\alpha\alpha\,Tay(7)} \rangle}{\langle S_{ZZXX,ZXZX,ZXXZ}^{\alpha\alpha\alpha\alpha\,Tay(7)} \rangle} \tag{32}$$

Equation (31) as a function of the internal angle between the two dipole moments, for different values of $\sqrt{\mu_\alpha \mu_\beta}\left(\frac{E^0}{\hbar}\right)$, is plotted in Fig. 8.

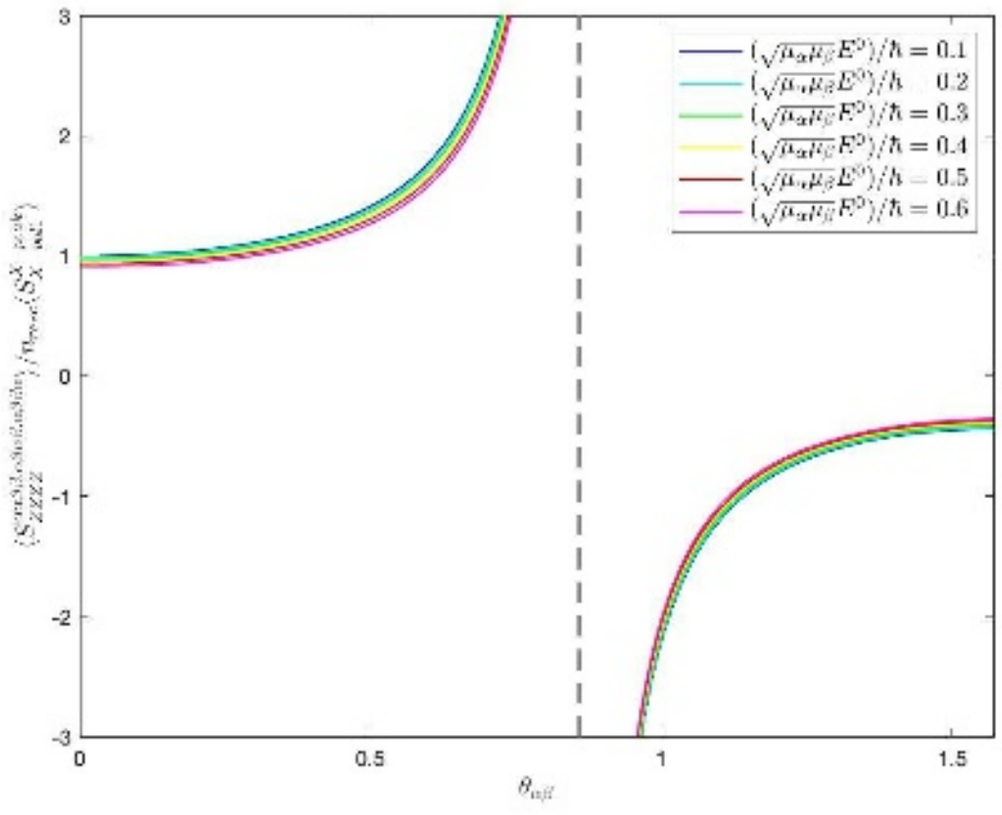

Fig. 8 Ratios between the rescaled ensemble averaged 7th order expansions of the signal for an all-parallel and a cross polarised cross peak as a function of the internal angle between the two transition dipoles, for increasing laser pulse electric field magnitudes.

Fig. 8 clearly shows how the orientational response of a cross peak has a dependence on the laser field magnitude. In other words, while the theory at the state of the art is a weak (zero)-field limit approximation of the polarization-resolved molecular response at the third order, the model here presented accounts for finite bleaching of the isotropic distribution of molecules in their ground state, prior to any laser-matter interaction. When strong illumination conditions are used, a broader angular distribution of dipoles around the field polarisation direction is excited, thus making the all-parallel and the cross-polarized polarization conditions resembling each other more and more as the laser field is increased. This effect translates to a field strength-dependent "flattening" of the signal ratio vs internal.

Because of this effect, not including intensity-dependent effects in the analysis of the orientational responses can lead to wrong assignment of the internal angle between two coupled transition dipoles. The same considerations apply to the analysis of transient anisotropy data, whose value can be computed combining the equations shown above, and are in agreement with the results obtained by Ansari for a two-pulse experiment.[48]

It has to be noted that our results have been derived in the approximation of a static ensemble of dipoles, thus not undergoing rotational diffusion. Although, the only time dependent variable used to model the field magnitude dependence on orientational responses in this contribution is the integrated laser field strength over the time duration of the pulse (Equation 3), during which the molecules are assumed to be static. Our model can then be modified to account for rotational diffusion contributions by including a signal decay due to dipole re-orientation and rotation in solution as shown by Hamm and Zanni[7] and Tokmakoff.[52]

Conclusions

Two-dimensional spectroscopies became an increasingly important tool to study energy and structural dynamics in the past decade. However, the investigation of non-trivial field-dependent effects on the measured signals have received surprisingly little attention.

In this contribution, we derived from first principles a formalism to calculate four-wave mixing signals.

Such method relies on an intermediate approach between perturbative and non-perturbative frameworks, in which an exact analytical expression to calculate four-wave mixing signals is shown in Eq. 8, but then the ensemble averaged values are obtained by integration over the solid angle of a Taylor series expansion, for weak field values.

Truncation of the Taylor series expansion at the lowest nonzero order reproduces perturbative results in literature, while including the nearest odd (thus nonzero) order (7th) of the same expansion allows to model the non-trivial laser pulse energy dependence of diagonal and cross peaks. Although, it has to be noted that including an upper order of the Taylor series expansion in the ensemble average integration does not mean that we are modeling six-wave mixing signals. Such term is included to model the effect of the pulse energy on the four-wave mixing signal.

These results have then been used to show how the pulse field strength can lead to finite bleach effects, which will modify the ratio between the rephasing all-parallel and cross-polarised signals of a cross peak, thus leading to wrong estimation of structural quantities in the molecular system under examination.

Although, it has to be noted that for values of electric field achievable by current tabletop laser amplifiers, the effects discussed in this contribution play a small role in the overall measured third-order molecular response.

Acknowledgments

G.B. and J.J. v T. acknowledge support from The Leverhulme Trust *via* award number RPG-2018-372. G.B. would like to thank Francesco Puccioni, Samuel Perrett and Alisia Fadini for the helpful discussions.

Data availability:

The data that support the findings of this study are available from the corresponding author upon reasonable request.

References

[1] D.M. Jonas, Annu. Rev. Phys. Chem. **54**, 425 (2003).
[2] S. Mukamel, *Principles of Nonlinear Optical Spectroscopy* (Oxford University Press, New York, 1995).
[3] T.A.A. Oliver, R. Soc. Open Sci. **5**, 171425 (2018).
[4] J. Cao, R.J. Cogdell, D.F. Coker, H.-G. Duan, J. Hauer, U. Kleinekathöfer, T.L.C. Jansen, T. Mančal, R.J.D. Miller, J.P. Ogilvie, V.I. Prokhorenko, T. Renger, H.-S. Tan, R. Tempelaar, M. Thorwart, E. Thyrhaug, S. Westenhoff, and D. Zigmantas, Sci. Adv. **6**, 4888 (2020).
[5] M. Cho, Chem. Rev. **108**, 1331 (2008).
[6] T. Brixner, R. Hildner, J. Köhler, C. Lambert, and F. Würthner, Adv. Energy Mater. **1700236**, 1 (2017).
[7] P. Hamm and M. Zanni, *Concepts and Methods of 2D Infrared Spectroscopy* (Cambridge University Press, Cambridge, 2011).
[8] Y.S. Kim and R.M. Hochstrasser, J. Phys. Chem. B **113**, 8231 (2009).
[9] P. Hamm, M. Lim, and R.M. Hochstrasser, J. Phys. Chem. B **102**, 6123 (1998).
[10] M. Khalil, N. Demirdöven, and A. Tokmakoff, J. Phys. Chem. A **107**, 5258 (2003).
[11] A. Ghosh, J.S. Ostrander, and M.T. Zanni, Chem. Rev. **117**, 10726 (2017).
[12] N.J. Hestand and F.C. Spano, Chem. Rev. **118**, 7069 (2018).
[13] E. Meneghin, F. Biscaglia, A. Volpato, L. Bolzonello, D. Pedron, E. Frezza, A. Ferrarini, M. Gobbo, and E. Collini, J. Phys. Chem. Lett. **0**, 7972 (2020).
[14] E. Meneghin, A. Volpato, L. Cupellini, L. Bolzonello, S. Jurinovich, V. Mascoli, D. Carbonera, B. Mennucci, and E. Collini, Nat. Commun. **9**, 1 (2018).
[15] E. Thyrhaug, K. Žídek, J. Dostál, D. Bína, and D. Zigmantas, J. Phys. Chem. Lett. **7**, 1653 (2016).
[16] L. Wang, M.A. Allodi, and G.S. Engel, Nat. Rev. Chem. (2019).
[17] L. Luer, V. Moulisova, S. Henry, D. Polli, T.H.P. Brotosudarmo, S. Hoseinkhani, D. Brida, G. Lanzani, G. Cerullo, and R.J. Cogdell, **109**, 1473 (2012).
[18] K. Hader, V. May, C. Lambert, and V. Engel, Phys. Chem. Chem. Phys. **18**, 13368 (2016).
[19] G. Bressan, D. Green, Y. Chan, P.C. Bulman Page, G.A. Jones, S.R. Meech, and I.A. Heisler, J. Phys. Chem. A **123**, 1594 (2019).
[20] G. Bressan, A. Cammidge, G. Jones, I. Heisler, D. González-Lucas, S. Remiro-Buenamañana, and S. Meech, J. Phys. Chem. A **123**, 5724 (n.d.).
[21] A. Halpin, P.J.M. Johnson, R. Tempelaar, R.S. Murphy, J. Knoester, T.L.C. Jansen, and R.J.D. Miller, Nat. Chem. **6**, 196 (2014).
[22] J.M. Richter, F. Branchi, F. Valduga De Almeida Camargo, B. Zhao, R.H. Friend, G. Cerullo, and F. Deschler, Nat. Commun. **8**, 1 (2017).
[23] F. V. A. Camargo, T. Nagahara, S. Feldmann, J. M. Richter, R. H. Friend, G. Cerullo, and F. Deschler, J. Am. Chem. Soc. **0**, (2020).
[24] E. Collini, H. Gattuso, L. Bolzonello, A. Casotto, A. Volpato, C.N. Dibenedetto, E. Fanizza, M. Striccoli, and F. Remacle, J. Phys. Chem. C **123**, 31286 (2019).
[25] G. Soavi, S. Dal Conte, C. Manzoni, D. Viola, A. Narita, Y. Hu, X. Feng, U. Hohenester, E. Molinari, D. Prezzi, K. Müllen, and G. Cerullo, Nat. Commun. **7**, 11010 (2016).
[26] R.E. Dale, J. Eisinger, and W.E. Blumberg, Biophys. J. **26**, 161 (1979).
[27] C. Fitzpatrick, J.H. Odhner, and R.J. Levis, J. Phys. Chem. A **124**, 6856 (2020).
[28] D.M. Jonas, Annu. Rev. Phys. Chem. **69**, 327 (2018).
[29] E. Meneghin, D. Pedron, and E. Collini, Chem. Phys. (2018).
[30] P. Bhattacharyya and G. R. Fleming, J. Phys. Chem. Lett. **10**, 2081 (2019).
[31] T.A.A. Oliver and G.R. Fleming, J. Phys. Chem. B **119**, 11428 (2015).
[32] D. Abramavicius, B. Palmieri, D. V. Voronine, F. Šanda, and S. Mukamel, Chem. Rev. **109**, 2350 (2009).
[33] D. Green, B.S. Humphries, A.G. Dijkstra, and G.A. Jones, J. Chem. Phys. **151**, (2019).
[34] G.D. Scholes, G.R. Fleming, L.X. Chen, A. Aspuru-Guzik, A. Buchleitner, D.F. Coker, G.S. Engel, R. van Grondelle, A. Ishizaki, D.M. Jonas, J.S. Lundeen, J.K. McCusker, S. Mukamel, J.P. Ogilvie, A. Olaya-

Castro, M.A. Ratner, F.C. Spano, K.B. Whaley, and X. Zhu, Nature **543**, 647 (2017).
[35] M.F. Gelin, D. Egorova, and W. Domcke, Acc. Chem. Res. **42**, 1290 (2009).
[36] J.J. Van Thor, J. Chem. Phys. **150**, (2019).
[37] R.W. Boyd, in *Nonlinear Opt.* (Elsevier, 2003), pp. 533–559.
[38] L.J.G.W. van Wilderen, C.N. Lincoln, and J.J. van Thor, PLoS One **6**, e17373 (2011).
[39] A. Ansari, C.M. Jones, E.R. Henry, J. Hofrichter, and W.A. Eaton, Biophys. J. **64**, 852 (1993).
[40] G. Bressan, M. Jirasek, H. Anderson, I. Heisler, and S. Meech, J. Phys. Chem. C **124**, 18416 (n.d.).
[41] L. Seidner, G. Stock, and W. Domcke, J. Chem. Phys. **103**, 3998 (1995).
[42] M.F. Gelin, B.J. Rao, M. Nest, and W. Domcke, J. Chem. Phys. **139**, 224107 (2013).
[43] H.S. Tan, J. Chem. Phys. **129**, (2008).
[44] A. Anda and J.H. Cole, J. Chem. Phys. **154**, 114113 (2021).
[45] I.. Ross, P. Matousek, M. Towrie, A.. Langley, and J.. Collier, Opt. Commun. **144**, 125 (1997).
[46] J. Kim, S. Mukamel, and G.D. Scholes, Acc. Chem. Res. **42**, 1375 (2009).
[47] L. Bolzonello, A. Volpato, E. Meneghin, and E. Collini, J. Opt. Soc. Am. B **34**, 1223 (2017).
[48] A. Ansari and A. Szabo, Biophys. J. **64**, 838 (1993).
[49] F.D. Fuller and J.P. Ogilvie, Annu. Rev. Phys. Chem. **66**, 667 (2015).
[50] R.M. Hochstrasser, Chem. Phys. **266**, 273 (2001).
[51] M. Lim, Bull. Korean Chem. Soc. **23**, 865 (2002).
[52] A. Tokmakoff, J. Chem. Phys. **105**, 1 (1996).

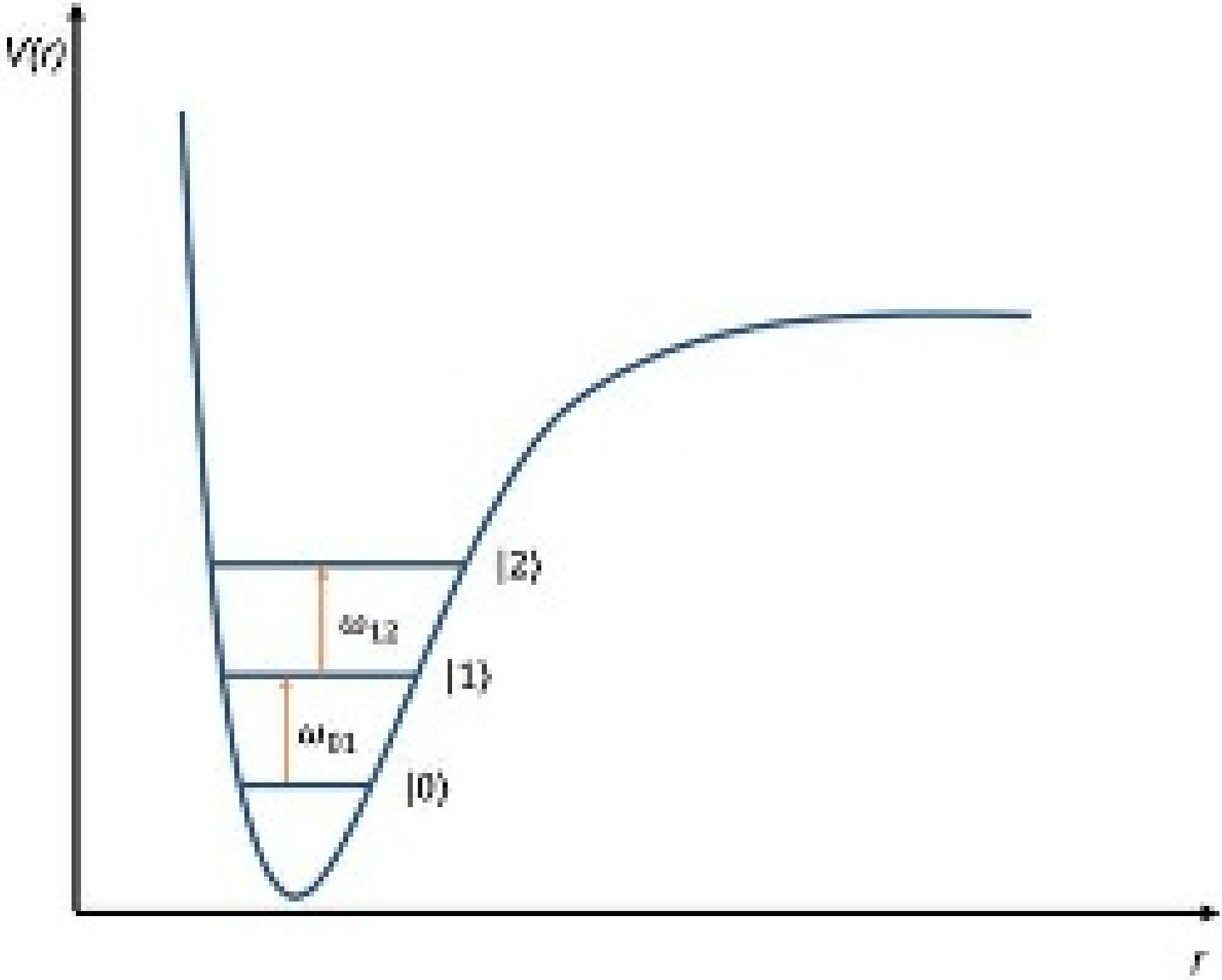
V(r)
|2⟩
ω21
|1⟩
ω10
|0⟩
r

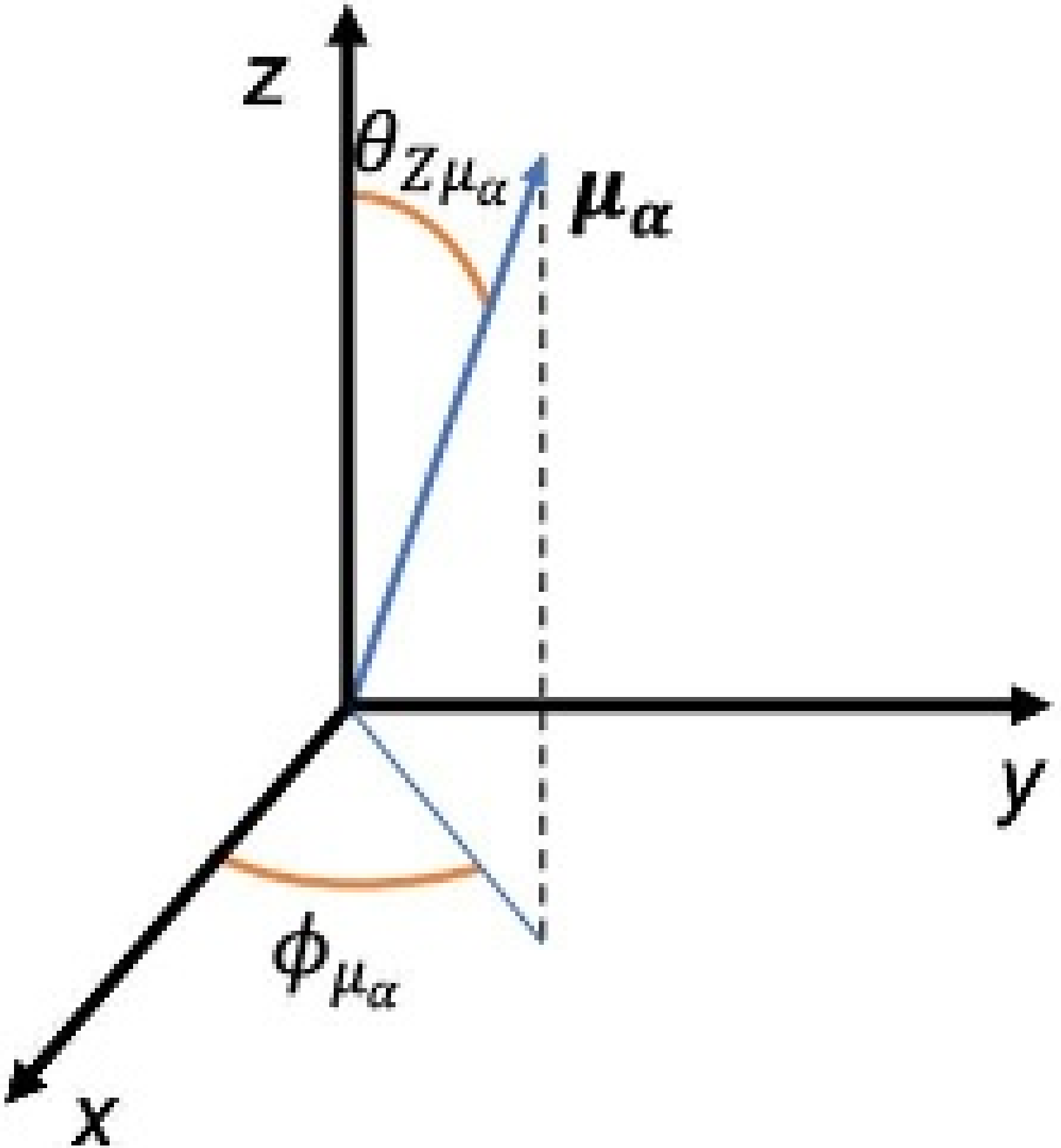
z
$\theta_{z\mu_\alpha}$
μ_α
y
ϕ_{μ_α}
x

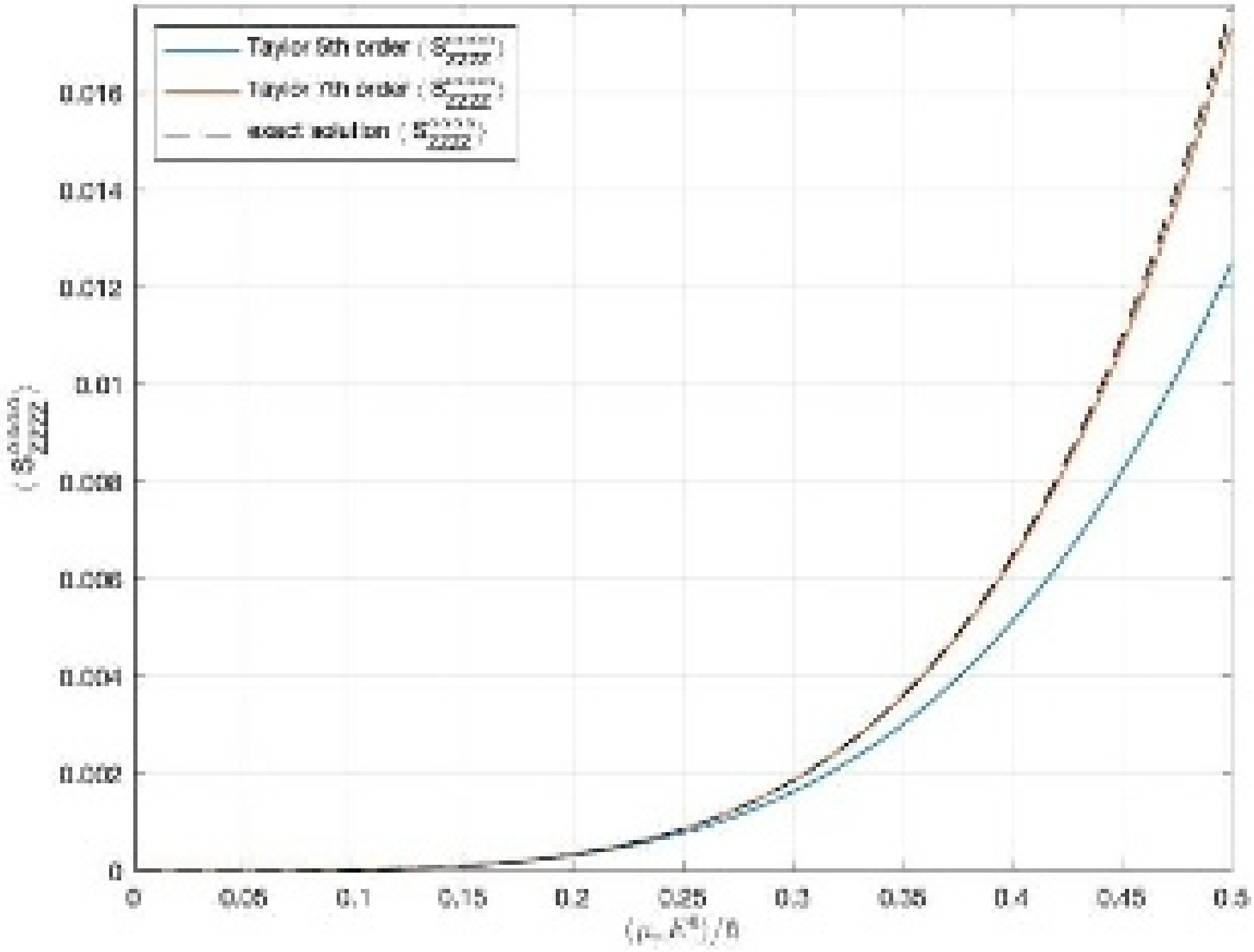
Taylor 6th order ($S^{(6)}_{zzzz}$)
Taylor 7th order ($S^{(7)}_{zzzz}$)
exact solution (S^{exact}_{zzzz})
0.018
0.016
0.014
0.012
0.01
0.008
0.006
0.004
0.002
0
$(S^{(6)}_{zzzz})$
0
0.05
0.1
0.15
0.2
0.25
0.3
0.35
0.4
0.45
0.5
$(\mu_0 A^2)/6$

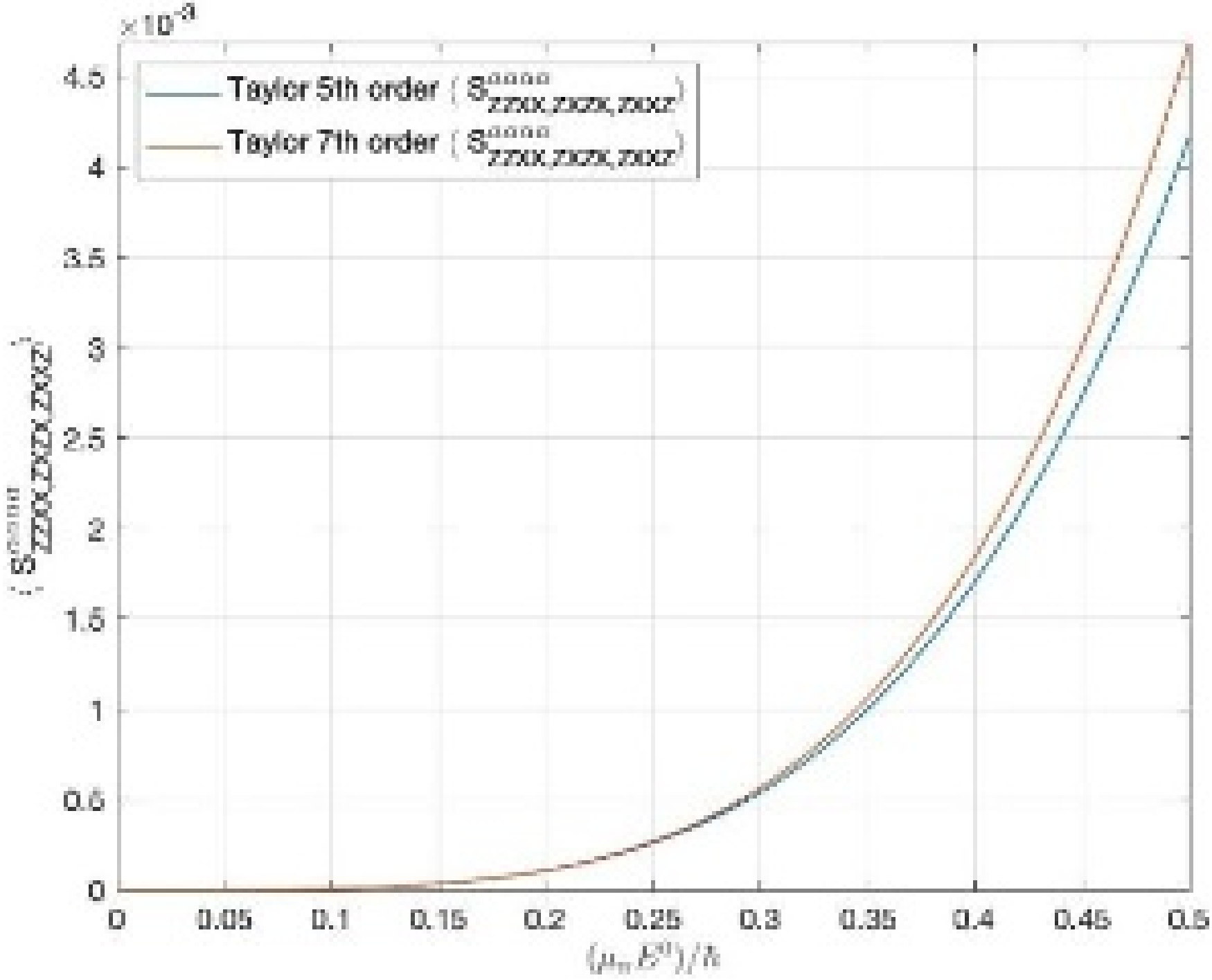
×10^-3
Taylor 5th order (S^55555_zzxx,zxzx,zxxz)
Taylor 7th order (S^55555_zzxx,zxzx,zxxz)
4.5
4
3.5
3
2.5
2
1.5
1
0.5
0
0
0.05
0.1
0.15
0.2
0.25
0.3
0.35
0.4
0.45
0.5
(μ_m E^0)/h

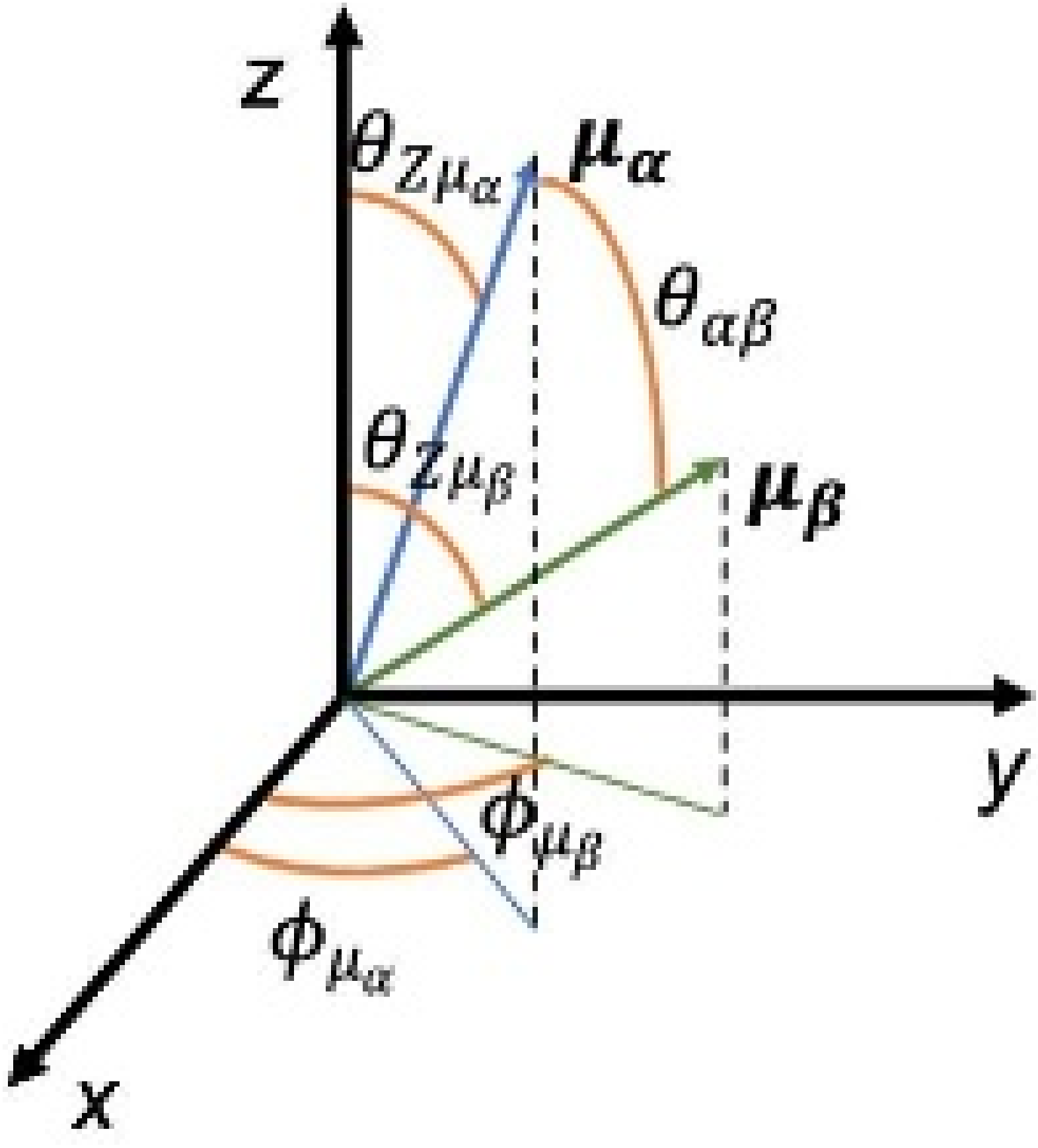
z
$\theta_{z\mu_\alpha}$
μ_α
$\theta_{\alpha\beta}$
$\theta_{z\mu_\beta}$
μ_β
y
$\phi_{y\mu_\beta}$
ϕ_{μ_α}
x

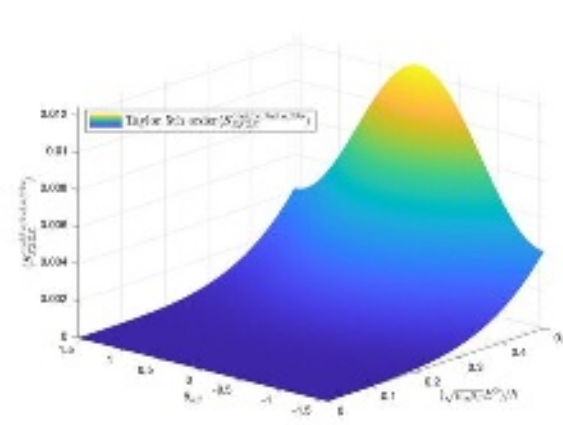
Taylor 5th order
0.012
0.01
0.008
0.006
0.004
0.002
0
0.1
0.2
0.3
0.4

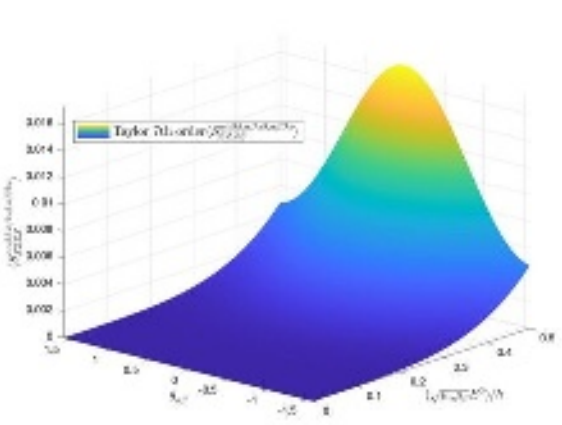
Taylor 5th order
0.016
0.014
0.012
0.01
0.008
0.006
0.004
0.002
0
0.1
0.2
0.3
0.4

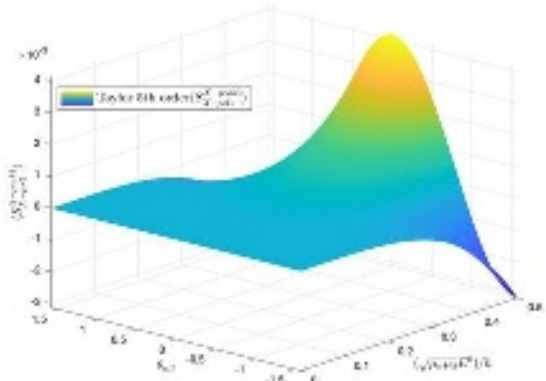

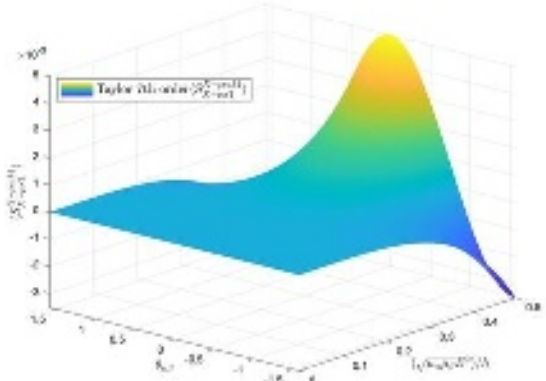

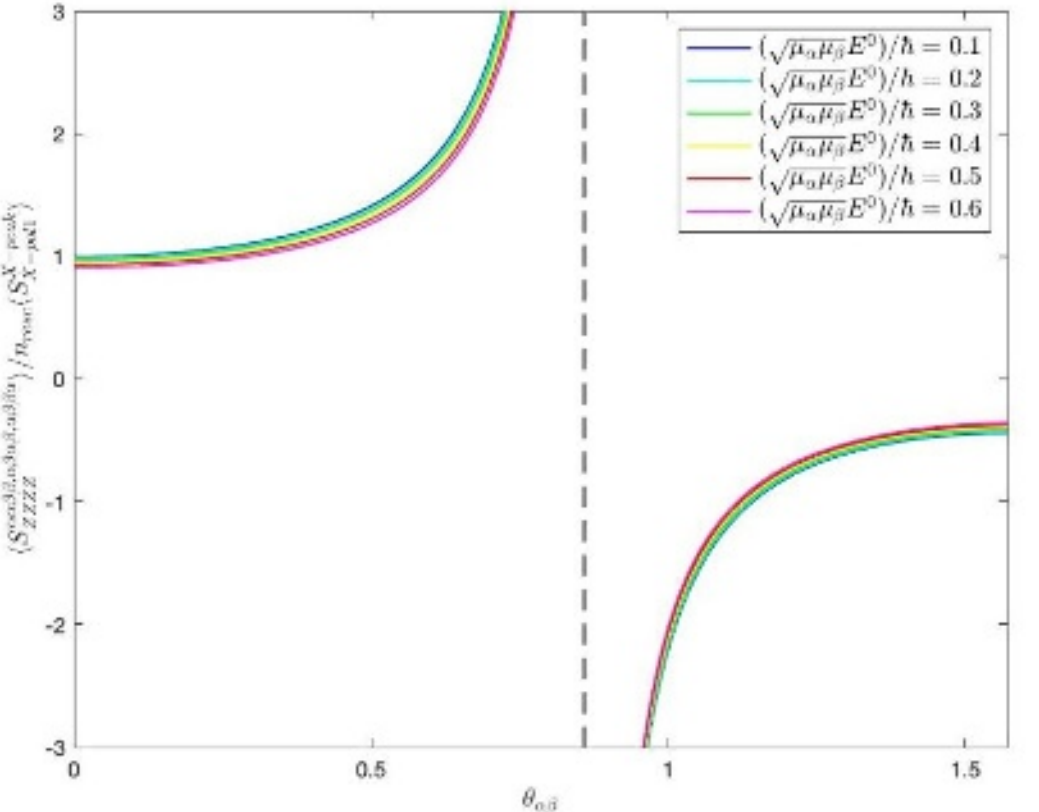
$(\sqrt{\mu_\alpha \mu_\beta} E^0)/\hbar = 0.1$
$(\sqrt{\mu_\alpha \mu_\beta} E^0)/\hbar = 0.2$
$(\sqrt{\mu_\alpha \mu_\beta} E^0)/\hbar = 0.3$
$(\sqrt{\mu_\alpha \mu_\beta} E^0)/\hbar = 0.4$
$(\sqrt{\mu_\alpha \mu_\beta} E^0)/\hbar = 0.5$
$(\sqrt{\mu_\alpha \mu_\beta} E^0)/\hbar = 0.6$
$(S^{\alpha\alpha\beta\beta,\alpha\beta\alpha\beta}_{ZZZZ})/\eta_{\mathrm{corr}}(S^{X-\mathrm{peak}}_{X-\mathrm{all}})$
$\theta_{\alpha\beta}$
3
2
1
0
-1
-2
-3
0
0.5
1
1.5